Microwave-initiated rapid synthesis of phthalated cashew gum for drug delivery systems

Antônia Carla de Jesus Oliveira (Formal analysis) (Methodology) (Investigation)<ce:contributor-role>Writing - Review and Editing) (Visualization) (Validation), Luíse Lopes Chaves<ce:contributor-role>Writing - Review and Editing) (Visualization) (Supervision), Fábio de Oliveira Silva Ribeiro (Methodology) (Formal analysis), Laís Ramos Monteiro de Lima (Methodology) (Formal analysis), Thaisa Cardoso de Oliveira (Methodology) (Formal analysis), Fátima García-Villén (Methodology) (Formal analysis), César Viseras (Methodology) (Investigation), Regina C.M. de Paula (Methodology)<ce:contributor-role>Formal Analysis), Pedro José Rolim-Neto (Methodology) (Formal analysis), Fernando Hallwass (Methodology) (Formal analysis) (Investigation)<ce:contributor-role>Data Curation)<ce:contributor-role>Writing - Review and Editing), Edson C. Silva-Filho (Methodology)<ce:contributor-role>Formal Analysis)<ce:contributor-role>Writing - Review and Editing), Durcilene Alves da Silva (Methodology) (Formal analysis)<ce:contributor-role>Writing - Review and Editing), José Lamartine Soares-Sobrinho (Conceptualization) (Validation) (Formal analysis) (Investigation)<ce:contributor-role>Writing - Review and Editing) (Visualization) (Supervision) (Resources) (Project administration), Mônica Felts de La Roca Soares (Conceptualization) (Validation) (Formal analysis) (Investigation)<ce:contributor-role>Writing - Review and Editing) (Visualization) (Supervision) (Resources) (Project administration)

PII: S0144-8617(20)31399-0

DOI: https://doi.org/10.1016/j.carbpol.2020.117226

Reference: CARP 117226

To appear in: *Carbohydrate Polymers*

Received Date: 6 June 2020

Revised Date: 28 September 2020

Accepted Date: 8 October 2020

Please cite this article as: Oliveira ACdJ, Chaves LL, Silva Ribeiro FdO, de Lima LRM, de Oliveira TC, García-Villén F, Viseras C, de Paula RCM, Rolim-Neto PJ, Hallwass F, Silva-Filho EC, Alves da Silva D, Soares-Sobrinho JL, de La Roca Soares MF, Microwave-initiated rapid synthesis of phthalated cashew gum for drug delivery systems, *Carbohydrate Polymers* (2020), doi: https://doi.org/10.1016/j.carbpol.2020.117226

Microwave-initiated rapid synthesis of phthalated cashew gum for drug delivery systems

Antônia Carla de Jesus Oliveira[1]; Luíse Lopes Chaves[1]; Fábio de Oliveira Silva Ribeiro[2]; Laís Ramos Monteiro de Lima[3]; Thaisa Cardoso de Oliveira[1]; Fátima García-Villén[4]; César Viseras [4,5]; Regina C. M. de Paula[3]; Pedro José Rolim-Neto[6]; Fernando Hallwass[7]; Edson C. Silva-Filho[8]; Durcilene Alves da Silva[2]; José Lamartine Soares-Sobrinho[1]; Mônica Felts de La Roca Soares[1]

[1]Quality Control Core of Medicines and Correlates – NCQMC, Department of Pharmaceutical Sciences, Federal University of Pernambuco, Recife, PE, Brazil.
[2]Research Center on Biodiversity and Biotechnology – BIOTEC, Federal University of Delta of Parnaiba, Parnaiba, PI, Brazil.
[3]Department of Organic and Inorganic Chemistry, Federal University of Ceara, Fortaleza, CE, Brazil.
[4]Department of Pharmacy and Pharmaceutical Technology, Faculty of Pharmacy, University of Granada, Granada, Spain.
[5]Andalusian Institute of Earth Sciences, CSIC – UGR, Armilla, Granada, Spain.
[6]Laboratory of Technology of Medicines – LTM, Federal University of Pernambuco, Recife, Brazil.
[7]Department of Fundamental Chemistry, Federal University of Pernambuco, Recife, PE, Brazil.
[8]Interdisciplinary Laboratory for Advanced Materials – LIMAV, Federal University of Piaui, Teresina, PI, Brazil.

Graphic abstract

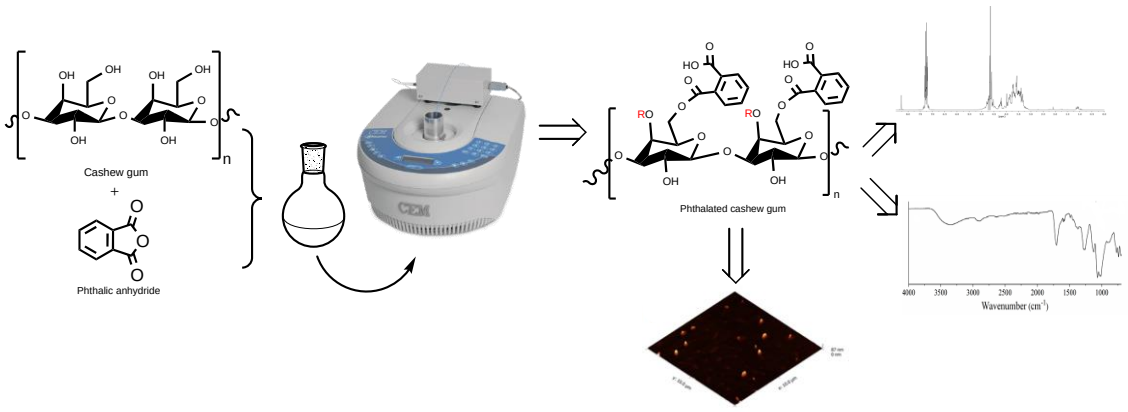

Highlights

- Phthalated cashew gum was synthesized by the microwave-initiated method.
- ^{1}H NMR spectroscopy was used to assess the degree of substitution of phthalated cashew gum.
- Modified phthalated cashew gum nanoparticles were developed for delivery of benznidazole.

Abstract

Chemical modification of polysaccharides is an important approach for their transformation into customized matrices that suit different applications. Microwave irradiation (MW) has been used to catalyze chemical reactions. This study developed a method of MW-initiated synthesis for the production of phthalated cashew gum (Phat-CG). The structural characteristics and physicochemical properties of the modified biopolymers were investigated by FTIR, GPC, ^{1}H NMR, relaxometry, elemental analysis, thermal analysis, XRD, degree of substitution, and solubility. Phat-CG was used as a matrix for drug delivery systems using benznidazole (BNZ) as a model drug. BNZ is used in the pharmacotherapy of Chagas disease. The nanoparticles were characterized by size, PDI, zeta potential, AFM, and *in vitro* release. The nanoparticles had a size of 288.8 nm, PDI of 0.27, and zeta potential of –31.8 mV. The results showed

that Phat-CG has interesting and promising properties as a new alternative for improving the treatment of Chagas disease.

Keywords: Polysaccharides; Chemical modification; Microwave irradiation; Polymeric nanoparticles; Benznidazole.

* Corresponding author at: Department of Pharmaceutical Sciences, Federal University of Pernambuco, Avenue Professor Arthur de Sá, s/n, 50740-521 - Cidade Universitária, Recife, Pernambuco, Brazil. E-mail address: joselamartine@hotmail.com (Soares-Sobrinho, J. L.).

1. Introduction

Biopolymers are a promising class of materials with a wide range of applications, of which health stands out, especially for use in the pharmaceutical field (Cordeiro et al., 2017). Characteristics such as biocompatibility, biodegradability, low toxicity, and low immunogenicity make these materials good candidates for application in drug delivery systems (DDS) (Pushpamalar et al., 2016). Biopolymers can be obtained from proteins (Jiang & Stenzel, 2016) and polysaccharides (Barclay et al., 2019).

Polysaccharides are high-performance macromolecular compounds obtained from renewable sources and found in almost all living organisms (Jacob et al., 2018). They are present in seeds, plant stems and leaves, animal body fluids, crustacean shells, and insects. They can also be extracted from cell walls and extracellular fluids of bacteria, yeast, and fungi (Garcia-Valdez, Champagne, & Cunningham, 2018).

Cashew gum (CG) is an exudate polysaccharide obtained from the stem of *Anacardium occidentale* L., which contains approximately 72% galactose, 14% glucose, 4–6% arabinose, 3–2% rhamnose, and 4–5% glucuronic acid (de Paula, Heatley, & Budd, 1998). It consists of a branched-chain polymer with bonds (1 → 6) β-D-galactose and (1 → 3) β-D-galactose (de Paula, & Rodrigues, 1995; de Paula, Heatley, & Budd, 1998). The attractive physical properties of CG allow its application in the food industry (Oliveira et al., 2020), odontology (Hasnain et al., 2018), and tissue engineering (Bal et al., 2020).

CG has high solubility in aqueous media; therefore, it can be used as a pharmaceutical excipient to design hydrophilic matrix tablets, promoting controlled drug delivery (Ofori-Kwakye et al., 2016). Its solubility can be altered by a chemical

modification process which can extend its application to carry drugs with low aqueous solubility (Abreu et al., 2016). The versatility of this material is related to the functional groups present in its chemical structure, especially to the primary hydroxyl group. These groups provide chemical reactivity for functionalization, which allows applications in DDS (Ribeiro et al., 2016; Subbiah, Veerapandian, & Yun, 2010).

Hydrophobization reactions in the CG structure allowed the production of new DDS that improved the rate of drug encapsulation as well as sustained delivery (Richter et al., 2020). Studies have promoted hydrophobization by the acetylation mechanism, using acetic anhydride, developed new systems for drug release with low water solubility, such as amphotericin B (Lima et al., 2018), indomethacin (Pitombeira et al., 2015; Cardial et al., 2019), and diethylammonium diclofenac (Dias et al., 2016).

Anhydrides are widely used in modification reactions because of the chemical environment offered by the OH groups of polysaccharides (Vasconcelos-Silva et al., 2019; Rodrigues et al., 2019). Ubaidulla et al. (2007) studied the derivatization of polysaccharides using phthalic anhydride. The obtained systems showed different physical and chemical properties, which were capable of increasing the applicability to DDS. In addition, the phthalated reaction has attracted attention to produce oral medication administration systems due to its low solubility in acidic medium, which protects the encapsulated drugs from the environmental stress and chemical/enzymatic digestion in gastric fluids (García-Casas et al., 2017). On the other hand, these systems are highly soluble in basic medium (Aiedeh et al., 2005).

Microwave (MW) irradiation has attracted attention as a methodology for the chemical modification of polysaccharides. Some of the advantages of MW-irradiation are clean product formation, reducing reaction time, and providing greater reaction control by decreasing the possible formation of byproducts, ensuring greater reproducibility of modified products (Singh, Kumar, & Sanghi, 2012). This methodology is an alternative to conventional thermal heating, which is a highly time-consuming process (Kumar et al., 2017; Desbrières, Petit, & Reynaud, 2014). For instance, MW-assisted synthesis of a new class of surfactants based on polysaccharides derived from polygalacturonic acid (PGA) was performed with a reaction time of 15 min, while the reaction under conventional thermal heating was carried out in 16 h (Mohd Aris et al., 2017). The MW-assisted reaction occurs when the polar molecules are exposed to the MW irradiation, and the molecules tend to align with the electric field of the MW. However, not all molecules are immediately aligned, generating

friction between the molecules and converting electromagnetic energy into thermal energy (Kalia, Sabaa, & Kango, 2013; Loupy, 2004). Bal et al. (2020) focused on the use of MW irradiation techniques to obtain polyacrylamide grafted cashew gum (CG-g-PAM) to create polymeric scaffolds for tissue growth.

Benznidazole (BNZ) is the main drug used for the treatment of Chagas disease (CD). CD is an infection caused by protozoan *Trypanosoma cruzi*, endemic in Latin America (Malik, Singh, & Amsterdam, 2015). According to the World Health Organization (WHO, 2010), CD is considered a neglected disease, and an important public health problem, with limited therapy. BNZ is commercially available as an immediate-release tablet. The treatment is administered 2 to 3 times a day for 60 days in most cases (Bermudez et al., 2016). However, the side effects limit its effectiveness and safety (García, Manzo, & Jimenez-Kairuz, 2018). In addition, BNZ has low aqueous solubility, which limits its bioavailability *in vivo* (Romero & Morilla, 2010). The literature cited the use of nanotechnology as a good strategy to improve the performance of BNZ (Santos-Silva et al., 2019; Seremeta et al., 2019).

This study evaluates the efficiency of MW irradiation in the preparation of CG with phthalic anhydride. In addition, phthalated cashew gum (Phat-CG) was used as a polymeric matrix for the development of BNZ-loaded nanoparticles for DDS.

2. Materials and Methods

2.1. Materials

Phthalic anhydride, cellulose acetate membrane (14000 Da), and deuterium oxide (D_2O) were obtained from Sigma-Aldrich (St. Louis, USA). Dimethyl formamide (DMF), acetone, sodium dodecyl sulfate (SDS), dimethyl sulfoxide (DMSO), and chloridric acid (HCl) were of analytical grade and obtained from Dinamica (SP, Brazil). The drug BNZ used in this study was donated by the Laboratory of the State of Pernambuco - LAFEPE (PE, Brazil).

2.2. CG Purification

Cashew exudate was collected from trees of the genus *Anacardium occidentale* L., native to Parnaiba, Piaui, Brazil. CG was purified using the method proposed by de Paula, Heatley, & Budd (1998).

2.3. Modification reaction

CG (1.0 g) and phthalic anhydride (2.0 g) in 10.0 mL DMF were irradiated in a microwave reactor (CEM Discover Microwave Reactor, USA). Three phthalated cashew gum (Phat-CG) derivatives were obtained: Phat-CG 1 (160 W, 3 min of reaction), Phat-CG 2 (250 W, 3 min of reaction), and Phat-CG 3 (250 W, 8 min of reaction). All experiments were performed at 80 °C. Phthalated derivatives were slowly precipitated with deionized water, and a solid whitish colored product was formed. Then, the precipitate was washed with water and dried in an oven at 50 °C.

2.4. Characterization of phthalated gum cashew

2.4.1. Fourier transform infrared spectroscopy (FTIR)

The FTIR spectra were obtained using a PerkinElmer Spectrum 400 (ATR) module in the range of 4000 to 700 cm^{-1}, combining 16 scans with a resolution of 4 cm^{-1}.

2.4.2. Gel permeation chromatography

Molar mass distribution was determined by gel permeation chromatography using a Shimadzu LC-20AD instrument coupled to a refractive index detector (RID - 10A). For the analysis, a 300 × 7.8 mm linear Polysep column was used with 0.1 mol/L $NaNO_3$ (aq) as the eluent. The measurement was performed at 30 °C, with a flow rate of 1 mL/min and the injected sample volume was 50 µL, using the following curve:

$$\mathrm{Log_M} = 14.33638 - 1.12336 \times \mathrm{V_e} \quad \text{Eq. (1)}$$

2.4.3. X-ray diffraction (XRD)

The crystallographic profile of the polysaccharides was determined using a PANalytical diffractometer (X'Pert Pro model) equipped with an X'Celerator solid-state detector and a spinning sample holder. The diffractogram patterns were recorded using randomly oriented mounts with CuKα radiation, operating at 45 kV and 40 mA, in the range of 2θ 4º to 70º.

2.4.4. Thermal analysis

Thermogravimetric analysis (TGA) was performed using a Shimadzu (mod. TGA-50H), equipped with a vertical oven and microbalance with a precision of 0.001

mg. Samples of CG and derivatives with approximately 10 mg were placed in aluminum crucibles and heated from 20 to 600 °C at 10 °C min^{-1} in a nitrogen atmosphere.

2.4.5. Elemental analysis

The elemental percentages of hydrogen and carbon were obtained using a PerkinElmer 2400 analyzer equipped with a thermal conductivity detector.

2.4.6. Nuclear magnetic resonance spectroscopy (^{1}H NMR)

Crude gum (30 mg) was dissolved in D_2O (0.7 mL). Phthalated derivatives (30 mg) were dissolved in D_2O (0.7 mL) basified with 1 M NaOH (10.0 μL). The spectra were obtained using an Agilent NMR spectrometer at 300 MHz. In order to suppress the residual water signal it was applied standard PRESAT pulse sequence.

The degree of substitution (DS) of the phthalated groups was calculated according to Eq. (2), where A is the integral area of the phthalated protons (7.11– 7.37 ppm), B is the integral area of 3.0 to 5.5 ppm, and n is the weighted average of the CG composition by the number of hydrogens, which do not undergo chemical exchange, in each monosaccharide (Vasconcelos Silva et al., 2019).

$$\mathrm{DS} = \frac{\mathrm{A}}{4} \times \frac{n}{\mathrm{B}} \qquad \text{Eq. (2)}$$

2.4.7. NMR relaxometry

The transverse relaxation time (T_2) was measured in the time domain, using a Minispec MQ-60 (Bruker, Germany) relaxometer, in the solid state of CG and phthalated derivatives.

2.4.8. Determination of solubility

CG and phthalated derivatives were dissolved in ultrapure water and in simulated gastric fluid (SGF) prepared according to USP34, without enzymes. All samples were a supersaturated state solution and were agitated for 24 h (Incubator SHAKER SL 222, SOLAB, SP, Brazil). This was followed by centrifugation at 2260 × g for 30 min (Excelsa II 206 - BL, Fanem, SP, Brazil). After drying in the oven at 50

°C, the resulting mass (recovered mass) was weighed. The experiments were performed tree times. The solubility was calculated using Eq. (3):

$$S = \frac{m \times 100}{m_i} \qquad \text{Eq. (3)}$$

$m = \text{ initial mass } (m_i) - \text{recovered mass}$

$S = \text{coefficient of solubility}$

2.5. Preparation and characterization of nanoparticles

2.5.1. BNZ nanoparticle preparation

The nanoparticles (NP-BNZ) were prepared following the nanoprecipitation technique (Chaves et al., 2018) with some modifications. Phat-CG 1 (20.0 mg) and BNZ (4.0 mg) were dissolved in 3.0 mL of acetone: DMSO (1:1 v/v). The aqueous phase, composed of ultrapure water (10.0 mL) (Elix® Advantage pure water, Merk, Darmstadt, Germany), was added to the organic phase and sonicated (Ultrasonic Tip Sonicator, Eco - sonics, SP, Brazil) for 2 min with 70% amplitude. Then, 10.0 mL of water were used as a stabilizer to complete the final volume of 20.0 mL of the solution.

The mixture was maintained under magnetic stirring at room temperature (25 °C) for the formation of nanoparticles, and complete evaporation of the organic solvent (Aminu, et al., 2013). Plain nanoparticles (without drug) were obtained by following the same procedure. All experiments were performed in triplicates.

2.5.2. Characterization of nanoparticles

Particle size, polydispersity index (PDI), and zeta potential measurements were performed using a Zetasizer Nano ZS (Malvern Instruments Ltd.), with a 633 nm laser. The particle size distribution was measured using dynamic light scattering (DLS). The zeta potential was determined by means of the electrophoretic mobility of the particles, and the measurements were performed in a folded capillary electrophoresis cell. The measurements were performed in triplicates at 25 °C, with a 90° detection angle.

The morphology of the nanoparticles was analyzed by atomic force microscopy (AFM) using a TT-AFM equipment (AFM Workshop, USA) in intermittent contact mode, using TED PELLA tips (TAP300 – G10) at an amplitude frequency of approximately 252.70 kHz. The samples were diluted at 1:100 in deionized water and left in an ultrasound bath for 15 min. After, a 10 µL aliquot of each sample was taken

and deposited on a mica surface and left for 15 min at room temperature to allow the sample to dry and then analyzed.

2.5.3. Encapsulation efficiency determination and drug loading

Quantitation of NP-BNZ was performed by determination of unencapsulated drug using the ultracentrifugation method. Briefly, the samples were prepared by diluting the nanoparticles with 0.1% (w/v) SDS, with pH adjusted to 3.5 (1 mol/L HCl).

The samples were centrifuged at 17,828 × g for 30 min (Centrifuge 5417R, Eppendorf). The supernatant absorbance was measured by UV-Vis spectroscopy (Vankel 50 UV-Vis, Varian) at 322 nm. A standard curve was obtained for BNZ at 0.1% (w/v) SDS. All analyses were performed in triplicates. The encapsulation efficiency (EE) and drug loading (DL) were calculated using Eq. (4) and Eq. (5).

$$\mathrm{EE} = \frac{\text{initial amount of drug} - \text{recovered drug}}{\text{initial amount of drug}} \text{ x } 100 \qquad \text{Eq. (4)}$$

$$\mathrm{DL} = \frac{\text{initial amount of drug} - \text{recovered drug}}{\text{initial amount of drug} + \text{ initial amount of polymer}} \text{ x } 100 \quad \text{Eq. (5)}$$

2.5.4. *In vitro* release study

Release profiles for NP-BNZ and free BNZ were obtained using a dialysis system. The nanoparticles were lyophilized, resuspended in 2.0 mL of water, introduced into the cellulose acetate membrane with a molecular weight cut-off of 14,000 Da and dialyzed against 50 mL of SGF without pepsin (USP 34) at 37 °C for 240 min under stirring (Incubator SHAKER SL 222, SOLAB, SP, Brazil).

At predetermined times (10, 20, 30, 45, 60, 120, and 240 min), samples of 0.6 mL were collected and quantified by UV-Vis spectroscopy. The fluid was replenished to keep the volume constant. The release profile of free BNZ was performed using the same parameters as for the nanoparticles. The analyses were performed in triplicates and the results expressed as mean ± S.D. Statistical analysis was performed using a two-way analysis of variance (ANOVA) followed by a post-hoc Tukey test ($p < 0.05$) using Prism Software Version 6 (Prism, Version 6, GraphPad Software Inc., La Jolla, CA, USA).

3. Results and discussion

3.1. Microwave-initiated modification reaction

In the present study, CG was modified using a MW-initiated synthesis method (Fig. 1). In this reaction, MW is absorbed by the polar OH groups linked to the polysaccharide, leading to the formation of favorable sites for modification (Desbrières et al., 2014). In addition, when using a polar solvent, such as DMF, which has a dielectric constant (*tan δ*: 0.161), the energy transfer to the phthalic anhydride molecules causes dielectric heating, producing another set of reactive sites. These effects generated in the polysaccharide chain and in phthalic anhydride recombine and promote the production of modified polysaccharides (Silva et al., 2012).

Phat-CG has been reported in previous studies (Lustosa et al., 2017; Oliveira et al., 2019). The process was carried out using a conventional method, which required high temperatures and was time-consuming. Reactions performed by MW present high performance at lower temperatures and shorter periods of reaction.

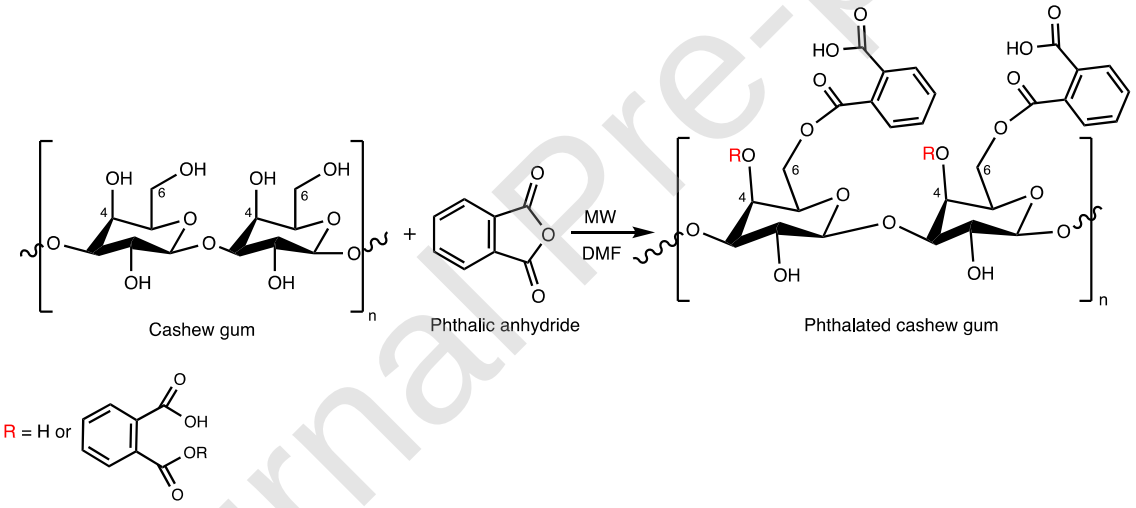

Fig. 1. Scheme of cashew gum phthalated modification.

3.2. Characterization of polysaccharides

Fig. 2 (A–D) shows the FTIR spectra of the CG and modified derivatives prepared under different conditions. The CG spectrum showed absorption bands around 3336, 2908, and 1015 cm^{-1}, showing the characteristic vibrations of O–H, C–H (carbon sp^3), and C–O–C (ether groups glycosidic), respectively (Silva Vasconcelos et al., 2019). For the reaction of CG in DMF, without phthalic anhydride, the MW heating method did not show substantial changes in the spectral pattern.

The FTIR spectra of CG and the modified derivatives showed small changes. However, the characteristic bands remained unchanged at 3358, 2902, and 1011 cm^{-1}, corresponding to O–H, C–H, and C–O–C, respectively. This similarity indicates that the effect of heating by MW did not change the primary structure of the CG.

New bands (in blue) emerged in the modified derivatives around 1710, and 1360 cm^{-1}, attributed to C=O and C–O stretching vibrations of carboxylic acid, respectively. The bands at 1630, 1602, and 1583 cm^{-1} can be assigned to the C=C bonds of the aromatic group. The two bands at 1284 and 1265 cm^{-1} can be attributed to the ester group (Lustosa et al., 2017). Comparing the FTIR spectrum obtained for the phthalation synthesized by conventional heating (Oliveira et al., 2019) and the spectra from Fig. 2, it was confirmed that the reaction using MW occurred successfully.

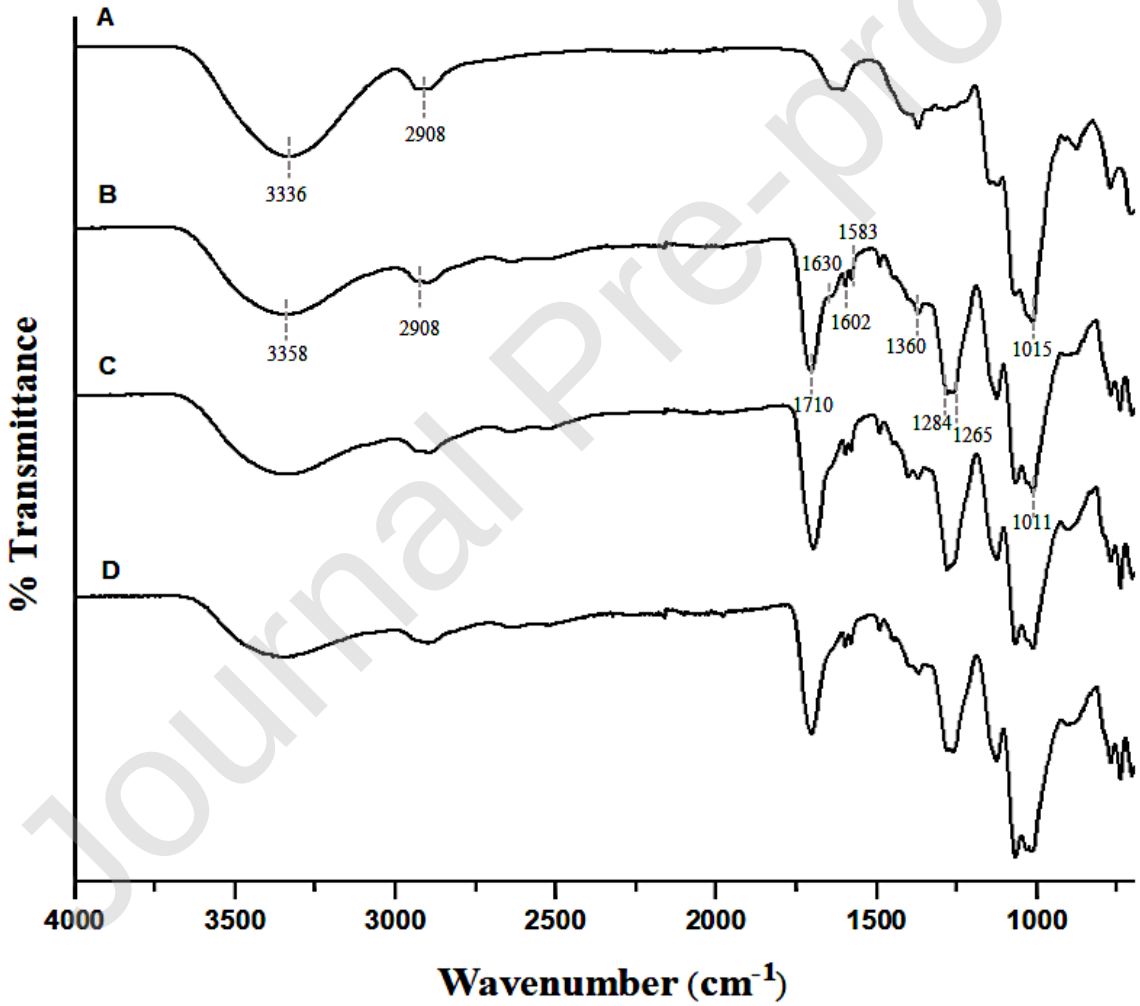

Fig. 2. FTIR spectra of (A) cashew gum, (B) phthalated cashew gum 1, (C) phthalated cashew gum 2 and (D) phthalated cashew gum 3.

The molecular weight of CG and phthalate derivatives were calculated and are shown in Table 1. The molecular weight of CG corresponds to that reported in the literature (Silva et al., 2019). It was observed that all derivatives showed a reduction in molecular weight. This is due to the polysaccharide modification process. When a polymeric chain is subjected to physical and chemical stress, inter- and intra-molecular bonds can be broken, decreasing molecular weight (Čížová et al., 2008). Phat-CG 3 showed a higher molecular weight compared to that of Phat-CG 2, probably due to exposure to greater power and reaction time. This is because under these conditions an increase in the reaction temperature may occur (Lewicka, Siemion, & Kurcok, 2015; Petit, Reynaud, & Desbrieres, 2015). The reactivity of OH groups tends to increase as the temperature increases; this phenomenon can cause cross-links in the polysaccharide, thus promoting greater molecular weight (Wang et al., 2014). In the study by Xing et al. (2004), MW radiation was performed to introduce N-sulfo and O-sulfo groups in chitosan. It has been observed that heating by MW is a convenient way to obtain a wide range of products with different molecular weight and DS, just by changing the irradiation time or energy conditions. This effect was observed for the reaction of the phthalated derivatives.

Table 1. Molecular weight, degree of substitution values and elemental analysis data from cashew gum and phthalated derivatives.

	Molecular weight (g/mol)	**DS**	**Carbon %**	**Hydrogen %**	**C (mmol)**	**H (mmol)**	**C/H**
CG	2.12×10^4		39.10	6.6	3.25	6.54	0.49
Phat-CG 1	7.38×10^3	0.31	45.80	5.97	3.81	5.92	0.64
Phat-CG 2	3.72×10^3	0.39	47.58	5.89	3.96	5.84	0.67
Phat-CG 3	1.22×10^4	0.43	47.18	5.88	3.92	5.83	0.67

The ^{1}H NMR spectra of CG and the modified derivatives are shown in Fig. 3 (A – D). CG and derivatives showed signals of the methyl group present in rhamnose at 1.3 and 1.1 ppm, respectively. The chemical shifts from 3.5 to 4.0 ppm correspond to H-2 to H-5. Signals at 4.3 and 4.8 indicate the H-1 of galactose and rhamnose, respectively. The chemical shift region from 4.6 to 5.0 refers to the anomeric protons (Vasconcelos Silva et al., 2019; Oliveira et al., 2019). The signals between 7.1 and 7.4 ppm (blue

arrow) represent the new signals that characterize the presence of the hydrogens of the aromatic ring inserted through the modification.

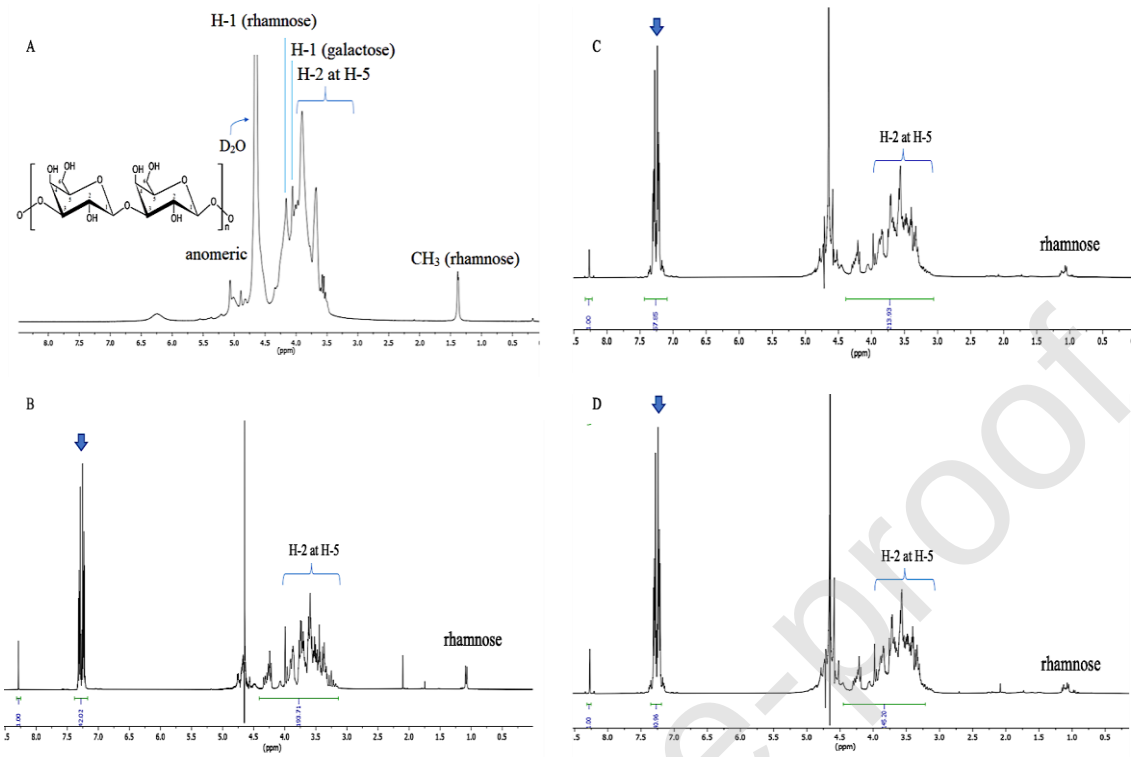

Fig. 3. ^{1}H NMR spectra of (A) cashew gum, (B) phthalated cashew gum 1, (C) phthalated cashew gum 2 and (D) phthalated cashew gum 3. For spectral B, C and D standard PRESAT pulse sequence was applied.

The results of the DS are shown in Table 1. The DS of the modified derivatives was calculated based on the integrals of the ^{1}H NMR spectra, according to Eq. 2 (Vasconcelos Silva et al., 2019). For the synthesis performed at 160 W for 3 min (Phat-CG 1), the DS was 0.31. The derivatives produced at 250 W showed DS values that varied from 0.39 and 0.43. In the study by Oliveira et al. (2019), where the modification was performed by the conventional heating method, a maximum DS value of 0.31 was obtained at a reaction time of 20 min. At the same CG/phthalic anhydride ratio (w/w) and increasing the reaction time to 8 min (Phat-CG3), an increase in the DS value (0.43) was observed.

Table 1 shows the results of the elemental analysis of CG and phthalic derivatives. An increase in the carbon and hydrogen (C/H) ratio compared to the CG with the modified derivatives was observed. This is due to the insertion of the

phthalated group into the polymer chain. However, the C/H ratio between the derivatives presented similar values, corroborating the results of DS by ^{1}H NMR.

Fig. 4 (A and B) shows the TG/DTG curves for the CG and phthalated derivatives. The first event in the region of 35–130 °C for CG was attributed to the loss of water and gas, where the percent loss was 8.08%. The second event for CG occurred at 214–265 °C, which corresponds to the condensation of hydroxyl groups. The third event for CG occurred at 269–345 °C, which corresponds to the thermal degradation of the polysaccharide structure with a loss of mass of 15.15% and 41.21%, respectively (Silva et al., 2006; Cordeiro et al., 2017).

For the Phat-CG 1 derivative, four degradation events were observed, with percentages of mass loss of 6.8% (34–108 °C), 4.78% (147–118 °C), 24.16% (195–263 °C) and 39.79% (272–337 °C). The derivatives Phat-CG 2 and Phat-CG 3 presented three degradation events. The percentages of mass loss for Phat-CG 2 were 6.23% (68–162 °C), 5.50% (172–337 °C), and 54.37% (208 –338 °C). For Phat-CG 3, the percentages of mass loss were 4.84% (62 –160 °C), 8.9% (166 –207 °C), and 56.0% (215 –333 °C). The first event observed for these derivatives showed lower values of moisture content when compared to CG. These data corroborated the values observed for the DS because as the derivative becomes more substituted, the water content decreases, changing the hydrophobicity of the material.

According to the TG/DTG curves, the second mass loss event of the derivatives was related to the phthalic anhydride grafted in the polysaccharide structure. It is possible to notice that the largest mass loss occurred with the derivatives that presented the highest DS value. Braz et al. (2018) studied the chemical modification of chitosan with maleic anhydride. They noted that while the DS increased, there was also an increase in the amount of variation of mass loss, as observed in this study with CG and phthalic anhydride.

The third and fourth decomposition events of Phat-CG 1 occurred at a temperature close to that observed for the second and third events of CG, which reveals that the thermal stability of this derivative has not been altered. On the other hand, the Phat-CG 2 and Phat-CG 3 derivatives presented similar decomposition profiles. It can be observed that the decomposition temperatures of these modified materials were lower than those of the CG, which reveals a lower thermal stability of the modified materials. When observing the degradation events of the Phat-CG 2 and Phat-CG 3 materials, one less event was identified when compared to the Phat-CG 1. However, a

shoulder was observed in the curves for Phat-CG 2 (212–266 °C) and Phat-CG 3 (215–266 °C), indicating overlap of these two events, which may have been caused by the amount of grafted material.

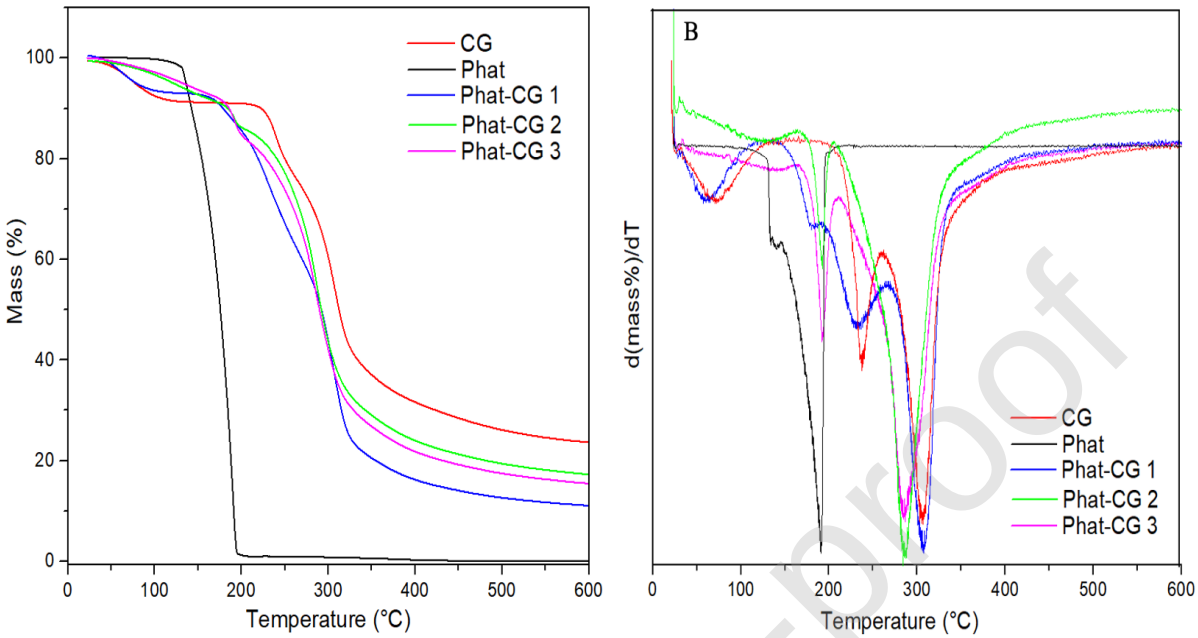

Fig. 4. Thermogravimetric curves (A) and derivative curves (B) of cashew gum and phthalated derivatives

Fig. 5 shows the diffractograms of the CG and phthalated derivatives. The CG showed amorphous characteristics because its structure follows a certain order of microcrystallinity (Vasconcelos Silva et al., 2019). The diffractograms of the derivatives showed new diffraction peaks at 2θ = 15.4°, 18.7°, 21.27°, 22.38°, 27.13°, 30.78°, 37.19°, and 37.86°. These changes reveal the incorporation of phthalic anhydride in the polymer chain, showing mixed characteristics of amorphicity and crystallinity. The modifications are expected to occur first in the hydroxyl groups, located on the surface of the polymer. After rearrangement of the surface, new crystallographic patterns may arise due to chemical interactions (Teixeira et al., 2018). All derivatives followed the same pattern of crystallinity; however, it was observed that the peak intensity increased with increasing DS.

Studies have reported that changes with anhydrides tend to increase the crystallinity of polysaccharides (Zang et al., 2013; Braz et al., 2018). This is a result of the possible interactions of phthalic anhydride with hydroxyl groups, and thus, these interactions affect the crystal growth process (Zhang & Zhang, 2015). After

modification, in general, rearrangements occur on the surface of the polysaccharides, and the appearance of new patterns suggests that they are π-π interactions (Melo et al., 2010). Aromatic rings are more prone to an organization process, and thus the molecular movements can be limited owing to their rigidity; therefore, the packaging of polymer chains in crystalline lattices is facilitated (Guimaraes et al., 2007).

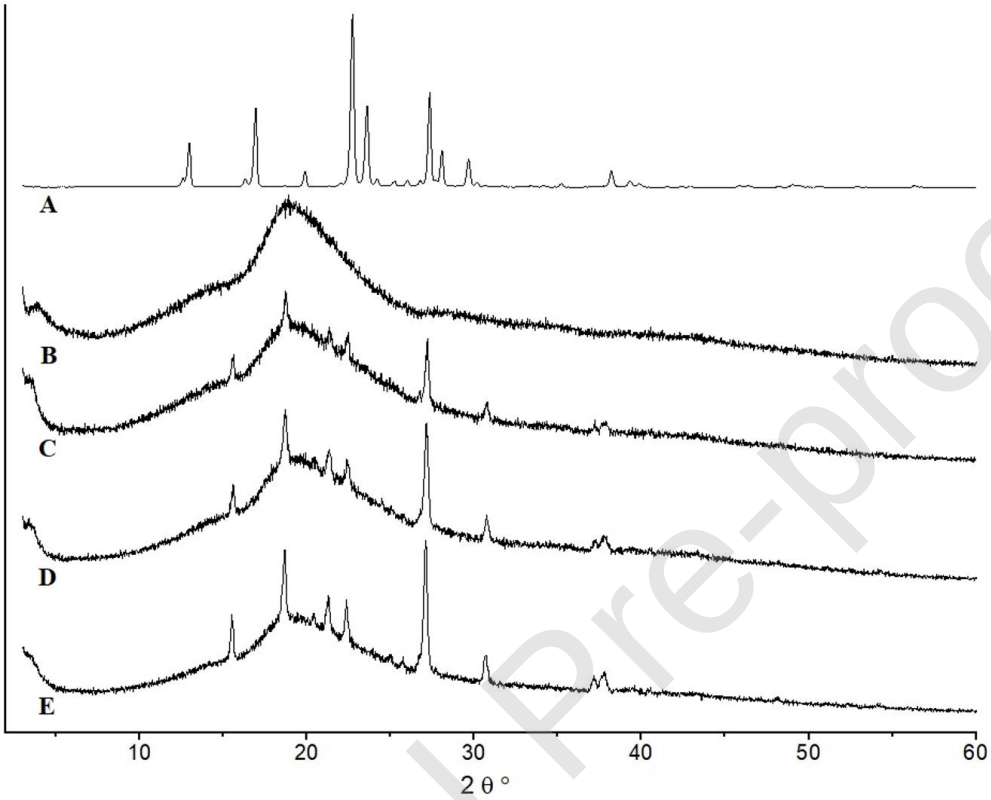

Fig. 5. X-ray diffraction patterns of (A) phthalic anhydride, (B) cashew gum, (C) phthalated cashew gum 1, (D) phthalated cashew gum 2 and (E) phthalated cashew gum 3.

Table 2. Solubility coefficient and relaxation time T_2 from cashew gum and phthalated derivatives.

	***T*₂ (ms)**	**Solubility g/100g H_2O**	**Solubility in SGF g/100g H_2O**
CG	0.42	94.47 ± 2.04	82.57 ±5.77
Phat-CG 1	0.15	27.56 ± 0.52	27.43 ± 3.57
Phat-CG 2	0.15	30.22 ± 3.52	30.31 ± 2.25
Phat-CG 3	0.15	26.33 ± 6.37	26.99 ± 4.86

Table 2 shows the results of NMR relaxometry experiments T_2. The T_2 measurements are correlated to the molecular dynamic of the polymer (Voron'koa et al., 2017). Compared to CG, the modified derivatives presented shorter T_2 times. This means that the phthalated derivatives showed less molecular mobility in structural terms. The presence of hydrophobic groups, which are related to the aromatic ring, guarantees the rigid domains and thus decreases the molecular mobility. These observations are easily corroborated by the crystallographic analysis, due to the crystalline profile phthalated derivatives present less mobility to the polymer chains (Shapiro, 2011).

Polysaccharides generally exhibit distinct structural characteristics in terms of molecular weight, composition, glycosidic binding pattern, and degree of branching (Gou et al., 2017). The study of these factors determines the functional properties of polysaccharides, such as solubility, which is critically important for various applications in pharmaceutical science (Vasconcelos Silva et al., 2019; Xu et al., 2019).

Table 2 shows the solubility coefficients of CG and phthalated derivatives in Milli-Q water and SGF without pepsin. In the literature, it is already defined that CG has good solubility in aqueous environments (Kim et al., 2018). This phenomenon is due to the presence of various OH groups, which leads to a strong interaction between polysaccharide molecules via hydrogen bonding. Therefore, the balance between polymer-water interactions is energetically favorable and creates a solvation layer around the polymeric chain that keeps the polysaccharide molecules apart (Mothé, & Rao, 1999; Nayak et al., 2019).

Due to the phthalated substituent, the modified derivatives exhibited low solubility in water. This effect is explained by the intramolecular interactions between the polymeric segments that cause aggregation between the polymeric chains, which hinders their solubility in aqueous media (Oliveira et al., 2019). The solubility results corroborate the other characterizations already discussed in this work, indicating that the insertion of the phthalated group occurred successfully in all derivatives. It was observed that the reaction in the MW occurred with the same efficiency under all reaction conditions. The solubility in SGF was evaluated with the purpose of using phthalated polymers as a possible polymeric matrix for drug transport. The literature

reports that the presence of phthalated groups under acidic conditions promotes drug protection (Aiedeh, Taha, & Al-Khatib, 2005; Ubaidulla et al., 2007).

3.3. Characterization of nanoparticles

Among the phthalated derivatives obtained, the Phat-CG 1 derivative was selected to produce nanoparticles. This derivative was chosen because it presented the closest pattern of thermal decomposition to that observed for CG, and the crystallinity peaks were less intense when compared to other derivatives. However, nanoparticles without the drug were obtained with all derivatives and characterized according to size, PDI, and zeta potential data. All presented similar characteristics. The method used to obtain the polymeric nanoparticles was nanoprecipitation. The polymer and the drug are in an organic phase that is miscible with water. When the aqueous phase is added to the organic phase, there is a decrease in the interfacial tension between the aqueous phase and the organic phase, and the diffusion of the organic solvent in the aqueous phase occurs very quickly, favoring the formation of nanoparticles (Sur et al., 2019). The sonication process contributed to a better particle size distribution (Karakus et al., 2019; Hedayati, Niakousari, & Mohsenpour, 2020).

The NP–BNZ presented average hydrodynamic size of 288.4 ± 8.5 nm, PDI of 0.27 ± 0.02 and zeta potential of –31.8 ± 0.9 mV, which are considered suitable parameters for monodisperse and stable nanosystems (Crucho, & Barros, 2017). The encapsulation efficiency and drug loading were 33.5% and 5.43%, respectively. Although suitable parameters have been achieved from the nanoparticles, it seems that encapsulation efficiency could be improved using optimization methods that improve the rates of drug loading (Santos-Silva et al., 2017). The nanoparticles without the drug presented a size of 270.3 ± 1.4 nm, PDI 0.26 ± 0.01 and zeta potential of –32.8 ± 1.8 mV. A slight increase in size was observed in NP–BNZ when compared to plain nanoparticles. This outcome corroborates other studies and can be explained by the presence of the drug that may rearrange the polymer matrix, providing an increase in size (Chaves et al., 2018; Aminu et al., 2020).

In the methodology discussed in this work, it was not necessary to use surfactant in the aqueous phase to obtain the polymeric systems. The polysaccharide obtained in our study has amphiphilic characteristics, which reduces the surface tension between the nanosystem and the aqueous solution, allowing the stabilization of the nanostructure (Mendes et al., 2011; Roy et al., 2014). This evidence can be seen from the zeta

potential analysis, which is an important parameter for particle stability (Abriata et al., 2017). The nanoparticles exhibited anionic character, due to the acid groups that were inserted in the CG chains. These results indicate that it may be advantageous to use a modified biopolymer instead of a synthetic polymer that has a high cost. Also, because of the high hydrophobicity of the synthetic polymer, it would be necessary the use of surfactants to improve the colloidal stability of the polymer system (Santos-Silva et al., 2017).

The morphology of the nanoparticles is shown in the AFM images of the NP-BNZ and unloaded nanoparticles (Fig. 6A–D). Both nanoparticles showed a spherical morphology. It was observed that the average sizes of the nanoparticles evaluated by AFM were smaller than those determined by DLS. The AFM analysis contains information on the three dimensions of the system. In the images, the z-axis is normally used to determine the diameter of spherical particles (Sitterberg et al., 2010; Eaton et al., 2017). The size analysis determined by DLS is an indirect measure, as the dimensions are evaluated by means of the hydrodynamic ray, measured from light scattering (Bhattacharjee, 2016). In addition, the ionic layers, solvation layer, and dispersion behavior of particles in solution are conditions that influence the measurement (Eaton et al., 2017).

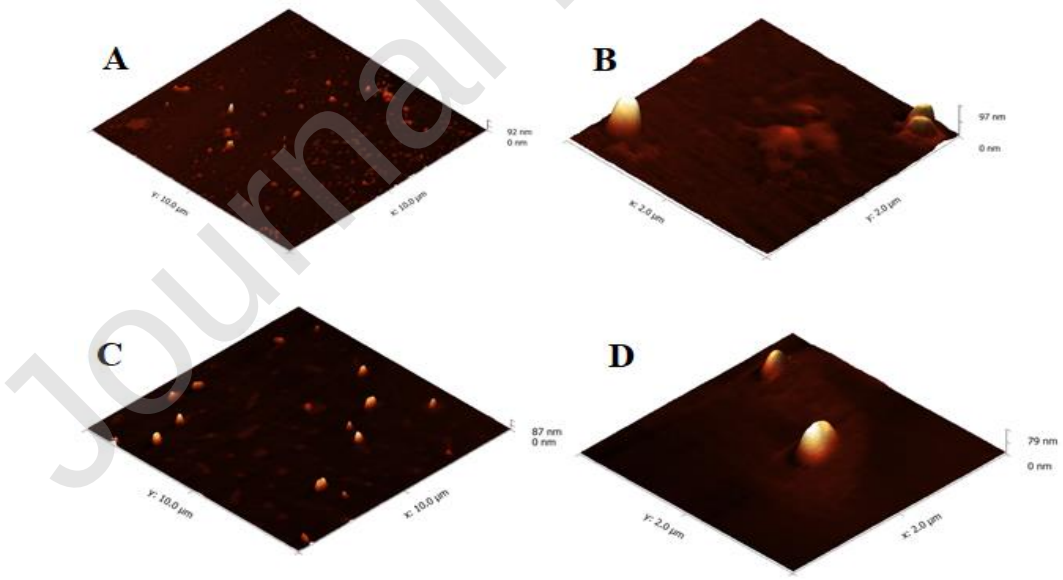

Fig.6. Atomic force microscopy 3D image of benznidazole-loaded nanoparticles (A-B) and nanoparticles without the drug (C-D). Images with a size range of 10 and 2 µm and a resolution of 512 pixels.

The *in vitro* release profile of NP-BNZ was studied to assess its performance as a form of oral administration. To accurately test a system's pH dependency, the *in vitro* release profile must simulate *in vivo* conditions (Asare-Addo, et al., 2011; Subbiah & Guldberg, 2019; Feng et al., 2020). The exposure time and the type of buffer must be representative and considered (Hu & Luo, 2018). The time and SGF used in this study were chosen, as they are the ones recommended to simulate gastric conditions (Gaucher et al., 2010; Wong, Al-Salami, & Dass, 2017). The release profile of free BNZ was also evaluated for comparative purposes. Fig. 7 shows the release profile of NP-BNZ and free BNZ under conditions of SGF without the presence of enzymes. As it can be seen, both NP-BNZ 8.6 ± 0.2% and free BNZ 8.7 ± 0.84% presented similar rates in the initial moments of release. This is because part of the BNZ remained on the surface of the nanoparticle (Seremeta et al., 2019). However, in 120 min, NP-BNZ released about 16.7 ± 2.3%, while for free BNZ 27.77 ± 4.1%. After 240 min, NP-BNZ released about 22.86 ± 1.2%, while for free BNZ 33.73 ± 4.5%. These differences were statistically significant with $p < 0.0001$. Compared to the free drug, the loaded NP-BNZ exhibited a continuous and considerably slower release.

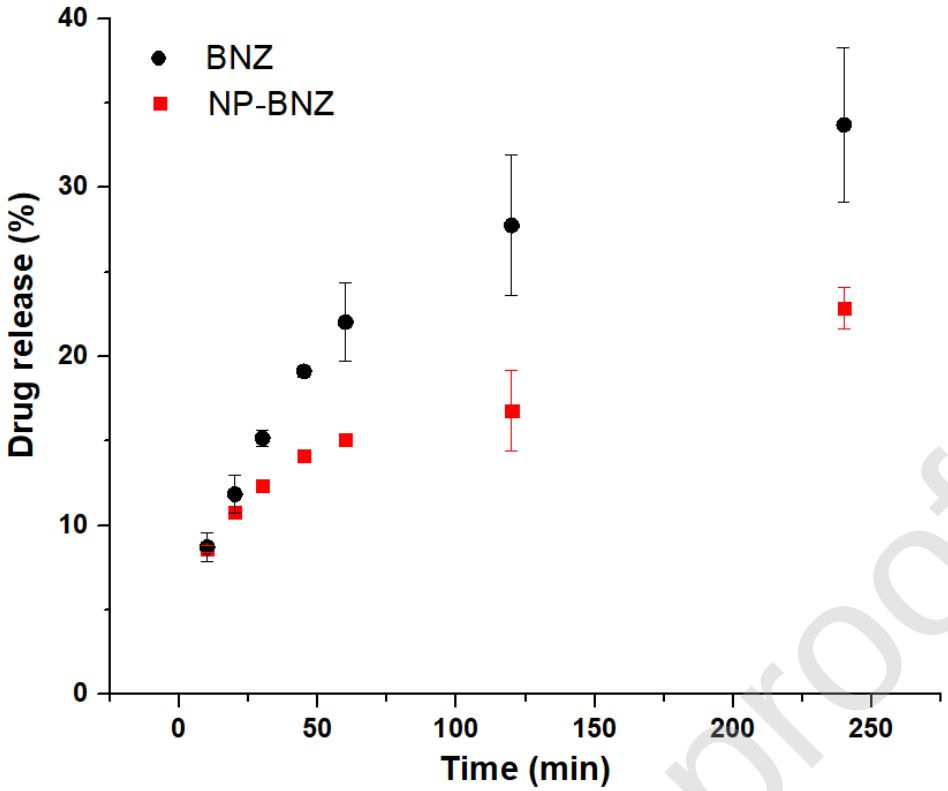

Fig. 7. *In vitro* release profile of benznidazole-loaded nanoparticles and free benznidazole at simulated gastric fluid.

This acid resistance of nanoparticles can be explained by the low swelling of the phthalated groups in the SGF medium, which was probably a result of the hydrophobic characteristics of the polymer. Under these conditions, the carboxylic groups present in the system are in a non-ionized form, which makes them less hydrophilic. García et al. (2018) showed the release profiles of BNZ in interpolyeletrolytic complexes composed of polysaccharides (chitosan and alginate) and synthetic polymers (polymethacrylates). For both systems, a slow and prolonged release of BNZ in the dissolution medium (SGF) was observed. In the case of the polysaccharide system, a lower BNZ release was observed compared to the polymethacrylate compound, due to the interactions between the amino groups of chitosan and the acid groups of alginate, since the solubility in the gastric medium of chitosan is avoided by the alginate network, which is insoluble under acidic conditions (Karuna et al., 2018).

The modified derivative used in this work can become an interesting platform for modified drug release, given its behavior for drug delivery systems using polysaccharides as a polymeric matrix. However, cytotoxicity tests and the evaluation of the effectiveness of nanoparticles in cell cultures for *T. cruzi* are still necessary.

4. Conclusion

In this study, a MW-initiated synthesis method to produce phthalate cashew gum was successfully performed. Three derivatives were prepared, and physicochemical characterization was performed. The variation in MW power and time influenced the properties of the derivatives. It was observed that the higher the MW power and time, the greater the hydrophobization of cashew gum. The temperature and magnetic agitation were maintained in a controlled manner to guarantee reproducibility and reliability of the results, showing that the methodology presented in this work is more efficient than the conventional thermal heating method. Using pharmaceutical technology as a strategy, it was possible to obtain polymeric nanoparticles using phthalated gum for BNZ administration. The results verified that, with the modification, the polymer provided greater protection to the drug in the simulated gastric fluid environment. Finally, the developed system can be useful for the treatment of Chagas disease.

CRediT authorship contribution statement

Antônia Carla de Jesus Oliveira: Formal analysis, Methodology, Investigation, Writing - Review & Editing, Visualization, Validation. **Luíse Lopes Chaves:** Writing - Review & Editing, Visualization, Supervision. **Fábio de Oliveira Silva Ribeiro:** Methodology, Formal analysis. **Laís Ramos Monteiro de Lima:** Methodology, Formal analysis. **Thaisa Cardoso de Oliveira:** Methodology, Formal analysis. **Fátima García-Villén:** Methodology, Formal analysis. **César Viseras:** Methodology, Investigation. **Regina C. M. de Paula:** Methodology, Formal Analysis. **Pedro José Rolim-Neto:** Methodology, Formal analysis. **Fernando Hallwass:** Methodology, formal analysis, Investigation, Data Curation, Writing - Review & Editing. **Edson C. Silva-Filho:** Methodology, Formal Analysis, Writing - Review & Editing. **Durcilene Alves da Silva:** Methodology, Formal analysis, Writing - Review & Editing. **José Lamartine Soares-Sobrinho:** Conceptualization, Validation, Formal analysis, Investigation, Writing - Review & Editing, Visualization; Supervision, Resources, Project administration. **Monica Felts de La Roca Soares:** Conceptualization, Validation, Formal analysis, Investigation, Writing - Review & Editing, Visualization; Supervision, Resources, Project administration.

Acknowledgments

The authors acknowledge Fundação de Amparo à Ciência e Tecnologia do Estado de Pernambuco (FACEPE) for a scholarship.

Declaration of Interest

The authors have no conflict of interest.

References

Abreu, C. M. W. S., Paula, H. C. B., Seabra, V., Feitosa, J. P. A., Sarmento, B., & de Paula, R. C. M. (2016). Synthesis and characterization of non-toxic and thermo-sensitive poly(N-isopropylacrylamide)-grafted cashew gum nanoparticles as a potential epirubicin delivery matrix. *Carbohydrate Polymers*, 154, 77-85.

Abriata, J. P., Eloy, J. O., Riul, T. B., Campos, P. M., Baruffi, M. D., & Marchetti, J. M. (2017). Poly-epsilon-caprolactone nanoparticles enhance ursolic acid *in vivo* efficacy against *Trypanosoma cruzi* infection. *Materials Science and Engineering C*, 77, 1196–1203.

Aiedeh, K. M., Taha, M. O., & Al-Khatib, H. (2005). Evaluation of chitosan succinate and chitosan phthalate as enteric coating polymers for diclofenac sodium tablets. *Journal of Drug Delivery Science and Technology*, 15, 207-211.

Aminu, N., Baboota, S., Pramod, K., Singh, M., Dang, S., Ansari, S. H., Sahni, J. K., & Ali, J. (2013). Development and evaluation of triclosan loaded poly-e-caprolactone nanoparticulate system for the treatment of periodontal infections. *Journal of Nanoparticle Research*, 15, 1-15.

Aminu, N., Chan, Y. S., Yam, M. F., & Toh, M. S. (2019). A dual-action chitosan-based nanogel system of triclosan and flurbiprofen for localised treatment of periodontitis. *International Journal of Pharmaceutics*, 570, 118659.

Asare-Addo, K., Levina, M., Rajabi-Siahboomi, R. A., & Nokhodchi, A. (2011). Effect of ionic strength and pH of dissolution media on theophylline release from

hypromellose matrix tablets—Apparatus USP III, simulated fasted and fed conditions. *Carbohydrate Polymers*, 86, 85-93.

Bal, T., Yadav, S. K., Rai, N., Swain, S., Shambhavi, Garg, S., & Sen, G. (2020). *In vitro* evaluations of free radical assisted microwave irradiated polyacrylamide grafted cashew gum (CG) biocompatible graft copolymer (CG-g-PAM) as effective polymeric scaffold. *Journal of Drug Delivery Science and Technology*, 56, 101572.

Barclay, T. G, Day, C. M., Petrovsky, N., & Garg, S. (2019). Review of polysaccharide particle-based functional drug delivery. *Carbohydrate polymers*, 221, 94-112.

Bermudez, J., Davies, C., Simonazzi, A., Real, J. P., & Palma, S. (2016). Current drug therapy and pharmaceutical challenges for Chagas disease. *Acta Tropica*, 156, 1–16.

Bhattacharjee, S. (2016). DLS and zeta potential - What they are and what they are not? *Journal of Controlled Release*, 235, 337–351.

Braz, E. M. A., Silva, S. C. C. C.; Silva, D. A., Carvalho, F. A. A., Barreto, H. M., Júnior, L. S. S., & Silva Filho, E. C. (2018). Modified chitosan-based bioactive material for antimicrobial application: Synthesis and characterization. *International Journal of Biological Macromolecules*, 117, 640-647.

Cardial, M. R. L., Paula, H. C. B., Silva, R B. C., Barros, J. F. S., Richter, A. R., Sombra, F. M., & De Paula, R. C. M. (2019). Pickering emulsions stabilized with cashew gum nanoparticles as indomethacin carrier. *International Journal of Biological Macromolecules*, 132, 534-540.

Chaves, L. L., Costa Lima, S. A., Vieira, A. C. C., Barreiros, L., Segundo, M. A., Ferreira, D., Sarmento, B., & Reis, S. (2018). Development of PLGA nanoparticles loaded with clofazimine for oral delivery: Assessment of formulation variables and intestinal permeability. *European Journal of Pharmaceutical Sciences*, 112, 28–37.

Čížová, A., Sroková, I., Sasinkova, V., Malovíková, A., & Ebringerova, A. (2008). Carboxymethyl Starch Octenylsuccinate: Microwave- and Ultrasound- assisted Synthesis and Properties. *Starch*, 60, 389- 397.

Cordeiro, M. S. F., Silva, C. M. B, Vieira, A. C. Q. M., Nadvorny, D., Sá, L. L. F., Souza, F. R. L., Nunes, L. C. C., Silva-Filho, E. C., Rolim-Neto, P. J., Veiga, F. B., Ribeiro, A. J., Soares, M. F. R., & Soares-Sobrinho, J. L. (2018). Biopolymers and

pilocarpine interaction study for use in drug delivery systems (DDS). *Journal of Thermal Analysis and Calorimetry*, 127, 1777-1785.

Crucho, C. I. C., & Barros, M. T. (2017). Polymeric nanoparticles: A study on the preparation variables and characterization methods. *Materials Science and Engineering C*, 80, 771-784.

de Paula, R. C. M., Heatley, F., & Budd, P. M. (1998). Characterization of *Anacardium occidentale* exudate polysaccharide. *Polymer International*, 45, 27–35.

de Paula, R. C. M., & Rodrigues, J. F. (1995). Composition and rheological properties of cashew tree gum, the exudate polysaccharide from *Anacardium occidentale* L. *Carbohydrate Polymers*, 26, 177–181.

Desbrières, J., Petit, C., & Reynaud, S. (2014). Microwave-assisted modifications of polysaccharides. *Pure and Applied Chemistry*, 86, 1695–1706.

Dias, S. F. L., Nogueira, S. S., Dourado, F. F., Guimarães, M. A., Pitombeira, N. A. O., Gobbo, G. G., Primo, F. L., Paula, R. C. M., Feitosa, J. P. A., Tedesco, A. C., Nunes, L. C. C, Leite, J. R. S. A., & Silva, D. A. (2016). Acetylated cashew gum-based nanoparticles for transdermal delivery of diclofenac diethyl amine. *Carbohydrate Polymers*, 143, 254–261.

Eaton, P., Quaresma, P., Soares, C., Neves, C., Almeida, M. P., Pereira, E., & West, P. (2017). A direct comparison of experimental methods to measure dimensions of synthetic nanoparticles. *Ultramicroscopy*, 182, 179–190.

Feng, K., Wei, S. Y., Hu, G. T., Linhardt, J. R., Zong, H. M., & Wu, H. (2020). Colon-targeted delivery systems for nutraceuticals: a review of current vehicles, evaluation methods and future prospects. *Trends in Food Science & Technology*, 102, 203-222.

García-Casas, I., Montes, A., Pereyra, C., & Martínez de La Ossa, E. J. (2017). Generation of quercetin/cellulose acetate phthalate systems for delivery by supercritical antisolvent process. *European Journal of Pharmaceutical Sciences*, 100, 79-86.

García, M. C., Guzman, M. L., Himelfarb, M. A., Litterio, N. J., Olivera, M. E., & Jimenez-Kairuz, A. (2018). Preclinical pharmacokinetics of benznidazole-loaded interpolyelectrolyte complex-based delivery systems. *European Journal of Pharmaceutical Sciences*, 122, 281–291.

García, M. C., Manzo, R. H., & Jimenez-Kairuz, A. (2018). Polysaccharides-based multiparticulated interpolyelectrolyte complexes for controlled benznidazole release. *International Journal of Pharmaceutics*, 545, 366–377.

Garcia-Valdez, O., Champagne, P., & Cunningham, M. F. (2018). Graft modification of natural polysaccharides via reversible deactivation radical polymerization. *Progress in Polymer Science*, 76, 151–173.

Gaucher, G., Satturwar, P., Jones, C-M., Furtos, A., & Leroux, J. C. (2010). Polymeric micelles for oral drug delivery. *European Journal of Pharmaceutics and Biopharmaceutics*, 76, 147-158.

Guimarães, D. H., Brioude, M. M., Fiúza, R. P., Prado, L. A. S. A., Boaventura, J. S., & José, N. M. (2007). Synthesis and characterization of polyesters derived from glycerol and phthalic acid. *Materials Research*, 10, 257-260.

Guo, M. Q., Hu, X., Wang, C., & Ai, L. (2017). Polysaccharides: Structure and Solubility. In Xu, Z. (Eds.), *Solubility of Polysacharides* (pp. 7-21). IntechOpen. eBook (PDF) ISBN: 978-953-51-4593-6.

Hasnain, M S., Rishishwar, P., Rishishwar, S., Ali, S., & Nayak, A. K. (2018). Extraction and characterization of cashew tree (Anacardium occidentale) gum; use in aceclofenac dental pastes. *International Journal of Biological Macromolecules*, 116, 1074-1081.

Hedayati, S., Niakousari, M., & Mohsenpour, Z. (2020). Production of tapioca starch nanoparticles by nanoprecipitation-sonication treatment. *International Journal of Biological Macromolecules*, 143, 136-142.

Hu, Q., & Luo, Y. (2018). Recent advances of polysaccharide-based nanoparticles for oral insulin delivery. *International Journal of Biological Macromolecules*, 120, 775-782.

Jacob, J., Haponiuk, J. T., Thomas, S., & Gopi, S. (2018). Biopolymer based nanomaterials in drug delivery systems: a review. *Materials Today Chemistry Journal*, 9, 43–55.

Jiang, Y., & Stenzel, M. (2016). Drug Delivery Vehicles Based on Albumin–Polymer Conjugates. *Macromolecular Bioscience*, 16, 791-802.

Kalia, S., Sabaa, M. W., & Kango, S. (2013). Polymer Grafting: A Versatile Means to Modify the Polysaccharides. In Kalia, S., & Sabaa, M. W. (Eds.), *Polysaccharide Based Graft Copolymers* (pp. 1-14). Berlin: Springer. Print ISBN: 978-3-642-36565-2.

Karakus, S., Ilgar, M., Kahyaoglu, M. I., & Kilislioglu, A. (2019). Influence of ultrasound irradiation on the intrinsic viscosity of guar gum–PEG/rosin glycerol ester nanoparticles. *International Journal of Biological Macromolecules*, 141, 1118-1127.

Karuna, D. S., Rathnam, G., Ubaidulla, U., Ganesh, M., & Jang, H. T. (2018). Chitosan phthalate: A novel polymer for the multiparticulate drug delivery system for diclofenac sodium. *Advances in Polymer Technology*, 37, 2013–2020.

Kim, S., Biswas, A., Boddu, V., Hwang, H., & Adkins, J. (2018). Solubilization of cashew gum from *Anacardium occidentale* in aqueous médium. *Carbohydrate Polymers*, 199, 205–209.

Kumar, D., Pandey, J., Raj, V., & Kumar, P. (2017). A review on the modification of polysaccharide through graft copolymerization for various potential applications. *The open medicinal chemistry journal*, *11*, 109–126.

Lewicka, K., Siemion, P., & Kurcok, P. (2015). Chemical modifications of starch: microwave effect. *International Journal of Polymer Science*, 2015, 1-10.

Lima, M. R., Paula, H. C. B., Abreu, F. O. M. S., da Silva, R. B. C., Sombra, F. M., & de Paula, R. C. M. (2018). Hydrophobization of cashew gum by acetylation mechanism and amphotericin B encapsulation. *International Journal of Biological Macromolecules*, 108, 523–530.

Loupy, A. (2004). Solvent-free microwave organic synthesis as an efficient procedure for green chemistry. *Comptes Rendus Chimie*, 7, 103–112.

Lustosa, A. K. M. F., Oliveira, A. C. J., Quelemes, P. V., Plácido, A., Silva, F. V., Oliveira, I. S., Almeida, M. P., Amorim, A. G. N., Deleure-Matos, C., Oliveira, R. C. M., Da Silva, D. A., Eaton, P. & Leite, J. R. S. A. (2017). *In situ* synthesis of silver nanoparticles in a hydrogel of carboxymethyl cellulose with phthalated-cashew gum as

a promising antibacterial and healing agent. *International Journal of Molecular Sciences*, 18, 2399.

Malik, L. H., Singh, G. D., & Amsterdam, E. A. (2015). Chagas Heart Disease: An Update. *American Journal of Medicine*, 128, 1251.

Melo, J. C. P., Silva-Filho, E. C., Santana, S. A. A., & Airoldi, C. (2010). Exploring the favorable ion-exchange ability of phthalylated cellulose biopolymer using thermodynamic data. *Carbohydrate Research*, 345, 13, 1914-1921.

Mendes, A. C, Baran, E. T., Nunes, C., Coimbra, M., Azevedo, H., & Reis R. L. (2011). Palmitoylation of xanthan polysaccharide for selfassembly microcapsule formation and encapsulation of cells in physiological conditions. *Soft Matter*, 7, 9647–9658.

Mohd Aris, Z. F., Bouldin, R. M, Pelletier, M. G. H., Gaines, P. Budhlall, B., & Nagarajan, R. (2017). Microwave-assisted synthesis and characterization of hydrophilically functionalized polygalacturonic acid. *Carbohydrate polymers*, 155, 432-439.

Mothé, C. G., & Rao, M. A. (1999). Rheological behavior of aqueous dispersions of cashew gum and gum arabic: effect of concentration and blending. *Food Hydrocolloids*, 13, 501-506.

Nayak, A. K., Ansari, M. T., Sami, F., Bera, H., & Hasnain, M. S. (2019). Cashew gum in drug delivery applications. In Hasnain, M. D. S. & Nayak, A. K. (Eds.), *Natural Polysaccharides in Drug Delivery and Biomedical Applications* (pp. 263-283). Academic Press, ISBN 9780128170557.

Ofori-Kwakye, K., Mfoafo, K. A., Kipo, S. L., Kuntworbe, N., & Boakye-Gyasi, M. E. (2016). Development and evaluation of natural gum-based extended release matrix tablets of two model drugs of different water solubilities by direct compression. *Saudi Pharmaceutical Journal*, 24, 82-91.

Oliveira, A. C. J., Araújo, A. R., Quelemes, P. V., Nadvorny, D., Soares-Sobrinho, J. L., Leite, J. R. S. A., Silva-Filho, E. C., & Da Silva, D. A. (2019). Solvent-free production of phthalated cashew gum for green synthesis of antimicrobial silver nanoparticles. *Carbohydrate Polymers*, 213, 176-183.

Oliveira, W. Q., Wurlitzer, N. J., Araújo, A. W. O., Comunian, T. A., Bastos, M. do S. R., Oliveira, A. L., Magalhães, H. C. R., Ribeiro, H. L., Figueiredo, R. W., & Sousa, P. H. M. (2020). Complex coacervates of cashew gum and gelatin as carriers of green coffee oil: The effect of microcapsule application on the rheological and sensorial quality of a fruit juice. *Food Research International*, 131, 109047.

Petit, C., Reynaud, S., & Desbrieres, J. (2015). Amphiphilic derivatives of chitosan using microwave irradiation. Toward an eco-friendly process to chitosan derivatives. *Carbohydrate Polymers*, 116, 26-33.

Pitombeira, N. A. O., Veras Neto, J. G., Silva, D. A., Feitosa, J. P. A., Paula, H. C. B., & de Paula, R. C. M. (2015). Self-assembled nanoparticles of acetylated cashew gum: Characterization and evaluation as potential drug carrier. *Carbohydrate Polymers*, 117, 610–615.

Pushpamalar, J., Veeramachineni, A. K., Owh, C., & Loh, X. J. (2016). Biodegradable Polysaccharides for Controlled Drug Delivery. *ChemPlusChem.*, 81, 504-514.

Ribeiro, A. J., De Souza, F. R. L., Bezerra, J. M. N. A., Oliveira, C., Nadvorny, D., De La Roca Soares, M. F., Nunes, L. C. C., Silva-Filho, E. C., Veiga, F., & Soares-Sobrinho, J. L. (2016). Gums' based delivery systems: review on cashew gum and its derivatives. *Carbohydrate Polymers*, 147, 188–200.

Richter, A. R., Carneiro, M. J., Sousa, N. A., Pinto, V. P. T., Freire, R. S., Sousa, J. S., Mendes, J. F. S., Fontenele, J. P. A., Paula, H. C. B., Goycoolea, F. M., & De Paula R. C. M. (2020). Self-assembling cashew gum-graft-polylactide copolymer nanoparticles as a potential amphotericin B delivery matrix. *International Journal of Biological Macromolecules*, 152, 492-502.

Rodrigues, J. A., Araújo, A. R., Pitombeira, N. A., Plácido, A., Almeida, M. P., Veras, L. M. C., Delerue-Matos, C., Lima, F. C. D. A., Batagin-Neto, A., de Paula, R. C. M., Feitosa, J. P. A., Eaton, P., Leite, J. R. S. A., & Da Silva, D. A. (2019). Acetylated cashew gum-based nanoparticles for the incorporation of alkaloid epiisopiloturine. *International Journal of Biological Macromolecules*, 128, 965-972.

Romero, E. L., & Morilla, M. J. (2010). Nanotechnological approaches against Chagas disease. *Advanced Drug Delivery Reviews*, 62, 576–588.

Roy, A., Comesse, S., Grisel, M., Hucher, N., Souguir, Z., Renou, F. (2014). Hydrophobically modified xanthan: an amphiphilic but not associative polymer. *Biomacromolecules*, 15, 1160–1170.

Santos-Silva, A. M., Caland, L. B., Oliveira, A. L. C. S. L., Araújo-Júnior, R. F., Fernandes-Pedrosa, M. F., Cornélio, A. M., & Silva-Junior, A. A. (2017). Designing structural features of novel benznidazole-loaded cationic nanoparticles for inducing slow drug release and improvement of biological efficacy. *Materials Science and Engineering C*, 78, 978–987.

Santos-Silva, A. M., Caland, L. B., Doro, P. N. M., Oliveira, A. L. C. S. L., Araújo-Júnior, R. F., Fernandes-Pedrosa, M. F., Egito, E. S. T., & Silva-Júnior, A. A. (2019). Hydrophilic and hydrophobic polymeric benznidazole-loaded nanoparticles: Physicochemical properties and *in vitro* antitumor efficacy. *Journal of Drug Delivery Science and Technology*, 51, 700-707.

Seremeta, K. P., Arrúa, E. C., Okulik, N. O., & Salomon, C. J. (2019). Development and characterization of benznidazole nano- and microparticles: A new tool for pediatric treatment of Chagas disease? *Colloids and Surfaces B: Biointerfaces*, 177, 169-177.

Shapiro, Y. E. (2011). Structure and dynamics of hydrogels and organogels: An NMR spectroscopy approach. *Progress in Polymer Science*, 36, 1184-1253.

Silva, A. M. G., Silva, V. L. M., Queirós, C., & Pinto, J. (2012). Avanços na síntese química: síntese assistida por micro-ondas. *Química*, 125, 61–69.

Silva, D. A., Feitosa, J. P. A., Maciel, J. S., Paula, H. C. B., & de Paula, R. C. M. (2006). Characterization of crosslinked cashew gum derivatives. *Carbohydrate Polymers*, 66, 16-26.

Silva, E. L. V., Oliveira, A. C. J., Silva-Filho, E. C., Ribeiro, A. J., Veiga, F., Soares, M. F. R., Wanderley, A. G., & Soares-Sobrinho, J. L. (2019). Nanostructured polymeric system based of cashew gum for oral administration of insulin. Revista *Matéria*, 24, e12399.

Singh, V., Kumar, P., & Sanghi, R. (2012). Use of microwave irradiation in the grafting modification of the polysaccharides - a review. *Progress in Polymer Science*, 37, 340–364.

Sitterberg, J., Özcetin, A., Ehrhardt, C., & Bakowsky, U. (2010). Utilising atomic force microscopy for the characterisation of nanoscale drug delivery systems. *European Journal of Pharmaceutics and Biopharmaceutics*, 74, 2-13.

Subbiah, R., & Guldberg, E. R. (2019). Materials science and design principles of growth factor delivery systems in tissue engineering and regenerative medicine. *Advanced Healthcare Mater*, 8, 1801000.

Subbiah, R., Veerapandian, M., & Yun, K. S. (2010). Nanoparticles: functionalization and multifunctional applications in Biomedical Sciences. *Current Medicinal Chemistry*, 17, 4559-4577.

Sur, S., Rathore, A., Dave, V., Reddy, R. K., Chouhan, S. R., & Sadhu, V. (2019). Recent developments in functionalized polymer nanoparticles for efficient drug delivery system. *Nano-Structures & Nano-Objects*, 20,100397.

Teixeira, P. R. S., Teixeira, A. S. N. M., Farias, E. A.O., Silva, D. A., Nunes, L. C. C., Leite, C. M. S., Silva-Filho, E. C. & Eiras, C. (2018). Chemically modified babassu coconut (*Orbignya* sp.) biopolymer: characterization and development of a thin film for its application in electrochemical sensors. *Journal of Polymer Research*, 25, 1-11.

Ubaidulla, U., Sultana, Y., Ahmed, F. J., Khar, R. K., & Panda, A. K. (2007). Chitosan phthalate microspheres for oral delivery of insulin: preparation, characterization, and *in vitro* evaluation. *Drug Delivery*, 23, 19-23.

Vasconcelos Silva, E. de L., Oliveira, A. C. de J., Patriota, Y. B. G., Ribeiro, A. J., Veiga, F., Hallwass, F., Silva-Filho, E. C., Silva, D. A., Soares, M. F. R., Wanderley, A. G., & Soares-Sobrinho, J. L. (2019). Solvent-free synthesis of acetylated cashew gum for oral delivery system of insulin. *Carbohydrate Polymers*, 207, 601–608.

Voron'koa, N. G., Derkacha, S. R., Vovkb, M. A., & Tolstoy, P. M. (2017). Complexation of k-carrageenan with gelatin in the aqueous phase analysed by ^{1}H NMR kinetics and relaxation. *Carbohydrate Polymers*, 169, 117–126.

Xing, R., Liu, S., Yu, H., Zhang, Q., Li, Z., & Li, P. (2004). Preparation of low-molecular-weight and high-sulfate-content chitosans under microwave radiation and their potential antioxidant activity *in vitro*. *Carbohydrate Research*, 339, 2515-2519.

Xu, Y., Wu, Y., Sun, P., Zhang, F., Linhardt, R. J., & Zhang A. (2019). Chemically modified polysaccharides: synthesis, characterization, structure activity relationships of action. *International Journal of Biological Macromolecules*, 132, 970-977.

Zhang, C., Han, B., Yao, X., Pang, L., & Luo, X. (2013). Synthesis of konjac glucomannan phthalate as a new biosorbent for copper ion removal. *Journal of Polymer Research*, 20, 1-14.

Zhang, X., & Zhang, Y. (2015). Poly (butylene succinate-co-butylene adipate)/cellulose nanocrystal composites modified with phthalic anhydride. *Carbohydrate Polymers*, 134, 52-59.

Wang, J., Yang, T., Tian, J., Zeng, T., Wang, X., Yao, J., Zhang, J., & Lei, Z. (2014). Synthesis and characterization of phosphorylated galactomannan: The effect of DS on solution conformation and antioxidant activities. *Carbohydrate Polymers*, 113, 325-335.

Wong, Y. C., Al-Salami, H., & Dass, R. C. (2017). Potential of insulin nanoparticle formulations for oral delivery and diabetes treatment. *Journal of Controlled Release*, 264, 247-275.

World Health Organization - WHO (2010). *Working to Overcome the Global Impact of Neglected Tropical Diseases - First WHO report on neglected tropical diseases*. Geneva: WHO Press, (Chapter 5).